J|A|C|S
ARTICLES
Published on Web 12/19/2001

A Joint Structural, Kinetic, and Thermodynamic Investigation of Substituent Effects on Host−Guest Complexation of Bicyclic Azoalkanes by β-Cyclodextrin

Xiangyang Zhang, Gabriela Gramlich, Xiaojuan Wang, and Werner M. Nau*

Contribution from the Department of Chemistry, University of Basel, Klingelbergstrasse 80, CH-4056 Basel, Switzerland

Received July 31, 2001

Abstract: Derivatives of the azoalkane 2,3-diazabicyclo[2,2,2]oct-2-ene (**1a**) with bridgehead 1,4-dialkyl (**1b**), 1,4-dichloro (**1c**), 1-hydroxymethyl (**1d**), 1-aminomethyl (**1e**), and 1-ammoniummethyl (**1f**) substituents form host−guest inclusion complexes with β-cyclodextrin. They were employed as probes to assess substituent effects on the kinetics and thermodynamics of this complexation by using time-resolved and steady-state fluorimetry, UV spectrophotometry, induced circular dichroism (ICD) measurements, and ^{1}H NMR spectroscopy. The kinetic analysis based on quenching of the long-lived fluorescence of the azoalkanes by addition of host provided excited-state association rate constants between 2.6×10^8 and 7.0×10^8 M^{-1} s^{-1}. The binding constants for **1a** (1100 M^{-1}), **1b** (900 M^{-1}), **1c** (1900 M^{-1}), **1d** (180 M^{-1}), **1e** (250 M^{-1}), and **1f** (ca. 20 M^{-1}) were obtained by UV, NMR, and ICD titrations. A positive ICD signal of the azo absorption around 370 nm was observed for the β-cyclodextrin complexes of **1a**, **1d**, and **1f** with the intensity order **1a** ≫ **1d** ≈ **1f**, and a negative signal was measured for those of **1b**, **1c**, and **1e** with the intensity order **1c** < **1b** ≈ **1e**. The ICD was employed for the assignment of the solution structures of the complexes, in particular the relative orientation of the guest in the host (co-conformation).

Introduction

Cyclodextrins (CDs) are naturally occurring water-soluble container-type host molecules.[1] Their host−guest complexes with organic guest molecules have application potential in catalysis,[2] photochemistry,[3] drug delivery,[4] and analytical chemistry.[5] In addition, they are attractive models for molecular recognition phenomena like enzyme−substrate or drug−target interactions.

Thermodynamic properties of CD complexes have been extensively studied.[6,7] In addition to thermodynamic data, knowledge of (1) the kinetics of host−guest complexation as well as (2) structural details is invaluable to assess the functionality of a particular host system and to develop structure−reactivity relationships in supramolecular chemistry in general. With respect to the latter aspect (2), crystallographic structures of several CD complexes have been obtained from X-ray and neutron diffraction data,[8] but relatively little is known about the solution structures of these complexes. NMR techniques have proven suitable to assess the depth of inclusion of the guest and to differentiate between inclusion and association complexes.[9] In addition, the induced circular dichroism (ICD) which arises from the interaction between an achiral chromophore with the chiral host molecules[6,7,10,11] has become a powerful tool for obtaining structural information on the relative orientation of the guest in the host, i.e., the so-called co-conformation.[12]

Relatively little is also known about aspect (1), i.e., the association and dissociation kinetics of guest molecules with CDs.[13] For exceptionally slow kinetics, the rate constants of CD complex formation can be assessed by stopped-flow methods[14,15] or NMR spectroscopy.[16,17] However, the inclusion of small guest molecules into CDs as well as other host structures with sufficiently large openings of the host cavity, e.g., calixarenes,[18] is typically a fast process with rate constants in the order of 10^7-10^8 M^{-1} s^{-1}. While such fast rate constants of supramolecular association may be desirable from certain application points of view, e.g., to allow high turnover rates in catalytic processes, their accurate determination presents an

(1) Szejtli, J. *Chem. Rev.* **1998**, *98*, 1743−1753.
(2) Takahashi, K. *Chem. Rev.* **1998**, *98*, 2013−2033.
(3) Bortolus, P.; Monti, S. *Adv. Photochem.* **1996**, *21*, 1−133.
(4) Uekama, K.; Hirayama, F.; Irie, T. *Chem. Rev.* **1998**, *98*, 2045−2076.
(5) Hedges, A. R. *Chem. Rev.* **1998**, *98*, 2035−2044.
(6) Connors, K. A. *Chem. Rev.* **1997**, *97*, 1325−1357.
(7) Rekharsky, M. V.; Inoue, Y. *Chem. Rev.* **1998**, *98*, 1875−1917.
(8) Harata, K. *Chem. Rev.* **1998**, *98*, 1803−1827.
(9) Schneider, H.-J.; Hacket, F.; Rüdiger, V.; Ikeda, H. *Chem. Rev.* **1998**, *98*, 1755−1785.
(10) Harata, K.; Uedaira, H. *Bull. Chem. Soc. Jpn.* **1975**, *48*, 375−378.
(11) Zhdanov, Y. A.; Alekseev, Y. E.; Kompantseva, E. V.; Vergeichik, E. N. *Russ. Chem. Rev. (Engl. Transl.)* **1992**, *61*, 563−575.
(12) Balzani, V.; Credi, A.; Raymo, F. M.; Stoddart, J. F. *Angew. Chem., Int. Ed.* **2000**, *39*, 3348−3391.
(13) Petrucci, S.; Eyring, E. M.; Konya, G. In *Comprehensive Supramolecular Chemistry*; Atwood, J. L., Ed.; Pergamon, New York, 1996; Vol. 8, pp 483−497.
(14) Yoshida, N. *J. Chem. Soc., Perkin Trans. 2* **1995**, 2249−2256.
(15) Abou-Hamdan, A.; Bugnon, P.; Saudan, C.; Lye, P. G.; Merbach, A. E. *J. Am. Chem. Soc.* **2000**, *122*, 592−602.
(16) Yim, C. T.; Zhu, X. X.; Brown, G. R. *J. Phys. Chem. B* **1999**, *103*, 597−602.
(17) Ghosh, M.; Zhang, R.; Lawler, R. G.; Seto, C. T. *J. Org. Chem.* **2000**, *65*, 735−741.
(18) Franchi, P.; Lucarini, M.; Pedulli, G. F.; Sciotto, D. *Angew. Chem., Int. Ed.* **2000**, *39*, 263−266.

10.1021/ja011866n CCC: $22.00

experimental challenge, since tailor-made probes (as guest molecules) and fast time-resolved techniques are required for their measurement. These include ultrasonic relaxation techniques,[19] temperature jump measurements,[20] and more frequently the absorption, emission, and quenching of triplet probes.[21,22] The latter has been recently reviewed.[23] Besides these direct spectroscopic methods, EPR line broadening was also exploited to examine the association kinetics for complexation of persistent nitroxide radicals with CDs.[24,25]

We have recently introduced a fluorescence-based method for assessing the kinetics of complexation by CDs.[26] In this photophysical method, 2,3-diazabicyclo[2.2.2]oct-2-ene (**1a**) is employed as a guest molecule, which serves also as a "dynamic" probe to monitor the kinetics of host−guest complexation by the fluorescence quenching inside the CD cavity. The exceedingly long-lived fluorescence of azoalkane **1a**, e.g., 730 ns in deaerated D_2O,[27,28] is the prerequisite for the direct measurement of absolute kinetic rate data by fluorescence, since the association process must occur within the lifetime of the excited state.[26] In addition to the kinetic measurements, azoalkane **1a** offered the possibility of thermodynamic measurements through several alternative methods, and it was also possible to assess the solution structure of the resulting CD complex by ICD.[29,30] The characteristic ICD of the n,π^* chromophore band around 370 nm depends sensitively on the alignment of this small chromophore within the CD complex, thus providing a unique tool for structure determination[29−32] in aqueous solution.

In this work, we employ bridgehead-substituted derivatives of the parent azoalkane **1a** as new probes to examine the effect of molecular structure of the guest molecule on the association rate constant and to compare it with the thermodynamics of association and the co-conformations of the host−guest complexes: 4-methyl-1-isopropyl-2,3-diazabicyclo[2.2.2]oct-2-ene (**1b**), 1,4-dichloro-2,3-diazabicyclo[2.2.2]oct-2-ene (**1c**), 1-hydroxymethyl-2,3-diazabicyclo[2.2.2]oct-2-ene (**1d**), and 1-aminomethyl-2,3-diazabicyclo[2.2.2]oct-2-ene in its neutral (**1e**) and protonated forms (**1f**) at pH 11 and pH 5, respectively. β-CD, which is composed of seven α-D-glucose units, was preferred over the smaller α-CD and the larger γ-CD forms, since it shows a 1−2 orders of magnitude stronger binding (e.g., for **1a**).[26,33,34]

Experimental Section

All commercial materials, including β-CD, were obtained from Fluka or Aldrich and were used as received. Column chromatography was performed on silica gel (60−200 μm). The azoalkane 2,3-diazabicyclo[2.2.2]oct-2-ene (**1a**)[35] and its derivatives **1b**,[29] **1c**,[36] **1d**,[37] and **1e**[38] were synthesized according to literature procedures. The detailed procedure and spectroscopic data for **1d**, which have not been previously reported, are given below. The azoalkanes were purified by sublimation at reduced pressure (not for **1d**) and subsequent 2-fold recrystallization from *n*-hexane (**1a**, **1b**, **1e**), methanol (**1c**), or diethyl ether (**1d**). D_2O (> 99.9%, Glaser AG, Basel, Switzerland) was used as solvent for all measurements.

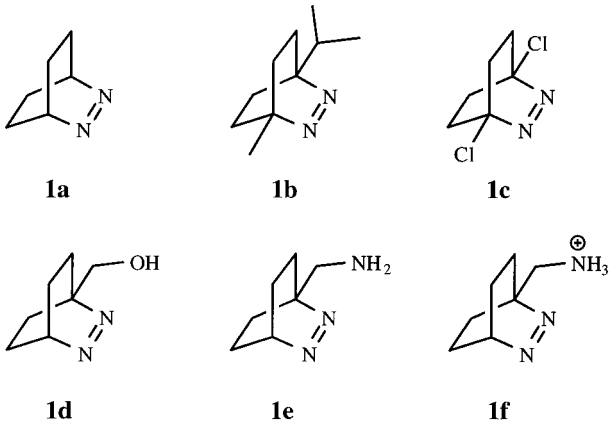

1a **1b** **1c** **1d** **1e** **1f**

1-(Hydroxymethyl)-2,3-diazabicyclo[2.2.2]oct-2-ene (1d). The starting material was the urazole 1-(hydroxymethyl)-4-methyl-2,4,6-triazatricyclo[5.2.2.0^{2,6}]undecane-3,5-dione, which was synthesized according to literature[37] from 2,3-dihydrobenzyl alcohol and 4-methylurazole and subsequent hydrogenation.[37] A 2.5 g (11.1 mmol) amount of the resulting urazole was dissolved in 50 mL of 2-propanol, and KOH pellets (4.8 g, 85.5 mmol) were added in small portions while stirring. After the solution was refluxed under argon for 15 h and cooled to room temperature, the solids were filtered off and washed with 2-propanol. Rotary evaporation of the filtrates gave a slurry which was suspended in CH_2Cl_2 and filtrated. After removal of solvent by rotary evaporation, the product was purified by silica gel chromatography (1.20 g, 8.55 mmol, 77%). Recrystallization from diethyl ether afforded colorless crystals of **1d** (mp 75−76 °C). UV (benzene): λ_{max} 380 nm, ϵ 220 cm^{-1} M^{-1}. ^{1}H NMR (400 MHz, $CDCl_3$): δ 1.33−1.79 (8 H, m, CH_2), 3.30 (1 H, s br, OH), 4.06 (2 H, s, CH_2OH), 5.25 (1 H, s br, CH). ^{13}C NMR (101 MHz, $CDCl_3$): δ 22.0 (2 C, CH_2), 23.3 (2 C, CH_2), 62.3 (CH), 67.3 (CH_2OH), 68.0 (C_q). Anal. Calcd for $C_7H_{12}N_2O$: C, 59.97; H, 8.63; N, 19.98; O, 11.41. Found: C, 60.14; H, 8.60; N, 20.04; O, 11.47.

Spectroscopic Measurements. All experiments were performed at ambient temperature in D_2O. For experiments with the amine form **1e** and the ammonium form **1f**, the pH values were adjusted to ca. 11 and 5 (by addition of NaOD or D_2SO_4) to bypass complications from the protonation equilibria, i.e., to work well below or above the pK_a value of the guest (pK_a = 9.2, see below), while avoiding deprotonation of the host, cf. pK_a(β-CD) = 12.34.[6] pH readings were taken from a 632 pH meter with a combined pH glass electrode (METROHM, Switzerland). Most spectroscopic experiments were performed in 4 mL cuvettes by using 3 mL of 4 mM stock solutions, except for **1c** (1.0 mM). Deaerated solutions, where required, were obtained by two *freeze−pump−thaw* degassing cycles using homemade quartz cells (4 × 1 × 1 cm) with high-vacuum Teflon stopcocks.

A XeF excimer laser pulse from a Lambda Physics COMPex 205 laser (351 nm, pulse width ca. 20 ns, pulse energy 40−175 mJ) or a

(19) Nishikawa, S.; Yokoo, N.; Kuramoto, N. *J. Phys. Chem. B* **1998**, *102*, 4830−4834.
(20) Cramer, F.; Saenger, W.; Spatz, H.-C. *J. Am. Chem. Soc.* **1967**, *89*, 14−20.
(21) Monti, S.; Flamigni, L.; Martelli, A.; Bortolus, P. *J. Phys. Chem.* **1988**, *92*, 4447−4451.
(22) Okano, L. T.; Barros, T. C.; Chou, D. T. H.; Bennet, A. J.; Bohne, C. *J. Phys. Chem. B* **2001**, *105*, 2122−2128.
(23) Bohne, C. *Spectrum* **2000**, *13* (3), 14−19.
(24) Kotake, Y.; Janzen, E. G. *J. Am. Chem. Soc.* **1992**, *114*, 2872−2874.
(25) Lucarini, M.; Luppi, B.; Pedulli, G. F.; Roberts, B. P. *Chem. Eur. J.* **1999**, *5*, 2048−2054.
(26) Nau, W. M.; Zhang, X. *J. Am. Chem. Soc.* **1999**, *121*, 8022−8032.
(27) Nau, W. M.; Greiner, G.; Rau, H.; Wall, J.; Olivucci, M.; Scaiano, J. C. *J. Phys. Chem. A* **1999**, *103*, 1579−1584.
(28) Nau, W. M. *J. Am. Chem. Soc.* **1998**, *120*, 12614−12618.
(29) Zhang, X.; Nau, W. M. *Angew. Chem., Int. Ed.* **2000**, *39*, 544−547.
(30) Mayer, B.; Zhang, X.; Nau, W. M.; Marconi, G. *J. Am. Chem. Soc.* **2001**, *123*, 5240−5248.
(31) Krois, D.; Brinker, U. H. *J. Am. Chem. Soc.* **1998**, *120*, 11627−11632.
(32) Bobek, M. M.; Krois, D.; Brinker, U. H. *Org. Lett.* **2000**, *2*, 1999−2002.
(33) Eftink, M. R.; Andy, M. L.; Bystrom, K.; Perlmutter, H. D.; Kristol, D. S. J. *J. Am. Chem. Soc.* **1989**, *111*, 6765−6772.
(34) Stoedeman, M.; Berg, U.; Svensson, A. *J. Chem. Soc., Faraday Trans.* **1998**, *94*, 1737−1741.
(35) Askani, R. *Chem. Ber.* **1965**, *98*, 2551−2555.
(36) Lüttke, W.; Schabacker, V. *Justus Liebigs Ann. Chem.* **1965**, *687*, 236−240.
(37) Engel, P. S.; Horsey, D. W.; Scholz, J. N.; Karatsu, T.; Kitamura, A. *J. Phys. Chem.* **1992**, *96*, 7524−7535.
(38) Hudgins, R. R.; Huang, F.; Gramlich, G.; Nau, W. M. *J. Am. Chem. Soc.*, in press.

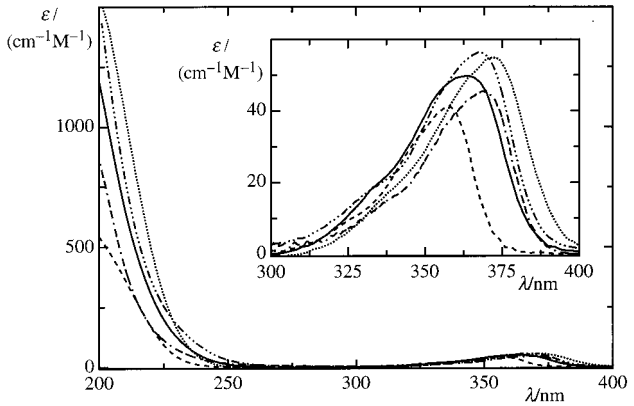

Figure 1. UV absorption spectra of azoalkane **1a** (—), **1b** (···), **1c** (- - -), **1d** (—···—), and **1e** (— —·— —), all in D_2O. The spectrum of **1f** is virtually superimposable with that of **1e** and is not shown for clarity. The inset shows the expanded spectra from 300 to 400 nm.

Table 1. Photophysical Properties of Azoalkanes **1** in D_2O, *n*-Hexane, and Their β-CD Complexes

	λ_{max}/nm [ϵ/(M^{-1} cm^{-1})]				τ/ns [deaerated][b]		
	D_2O	*n*-hexane	β-CD·**1**	λ_{iso}/ nm[a]	D_2O (τ_0)	*n*-hexane	β-CD·**1** (τ_{CD})[c]
1a	365 [48]	376 [200]	371	358	505 [730]	[340]	80
1b	373 [54]	383 [200]	379	376	590 [810]	[770]	430
1c	358 [40]	367 [190]	364	356	705 [750]	[30]	40
1d	368 [54]	380 [140]	370	371	565 [840]	[335]	95
1e	369 [43]	381 [120]	373	371	660 [880]	[420]	110
1f	370 [43]	*d*	370[e]	(370)[e]	670 [920]	*d*	75

[a] Isosbestic point in the UV titration by β-CD in D_2O. [b] Fluorescence lifetime in aerated [deaerated] solution; 5% error. [c] Fluorescence lifetime in the β-CD complex in aerated D_2O obtained by simultaneous fitting of the time-resolved and steady-state fluorescence data according to eqs 6 and 9; 10% error. [d] Insoluble in *n*-hexane. [e] No significant UV shift was observed upon addition of β-CD.

Continuum Minilite Nd:YAG laser (355 nm, pulse width 3−7 ns, 7 mJ) was used for excitation to obtain the time-resolved fluorescence decays. The decays were monitored with a monochromator−photomultiplier setup at 420−500 nm, depending on signal intensity. The kinetic traces were registered by means of a transient digitizer and analyzed by nonlinear least-squares fitting of monoexponential or biexponential decay functions, where appropriate. Steady-state fluorescence spectra were measured with a Spex Fluorolog fluorimeter or with an FLS900 setup from Edinburgh Instruments. Steady-state fluorescence quenching experiments with β-CD were performed with excitation at the isosbestic points (λ_{iso}) which were obtained from UV titrations. UV spectra were obtained with a Hewlett-Packard 8452 diode array spectrophotometer (2 nm resolution) or with a Perkin-Elmer Lambda 19 spectrophotometer (0.1 nm resolution). The NMR spectra were obtained with a Bruker DPX 400 MHz Avance NMR spectrometer. Induced circular dichroism spectra were recorded with a Jasco J-720 spectropolarimeter (0.2 nm resolution, 25 accumulations, 1 cm cell) or an AVIV circular dichroism spectrometer (model 62A DS, Lakewood, NJ).

Results

Photophysical Properties. The UV spectra of **1a**−**f** in D_2O are quite similar (Figure 1). The substituents have only a minor effect on the n,π* transition near 370 nm (Table 1), causing a slight bathochromic shift for electron-donating groups (**1b**) and a hypsochromic one for electron-withdrawing groups (**1c**). A substituent-dependent shift was also observed for the π,π* transition[30] below 220 nm (Figure 1).

Table 2. Binding Constants, ICD Ellipticities, and Association Rate Constants of the β-CD Complexes of Azoalkanes **1**

guest	K/M^{-1}[a]	θ/mdeg[b]	$\Delta\epsilon$/ (M^{-1} cm^{-1})[c]	k_{ass}/ 10^8 M^{-1} s^{-1}[d]	k_{diss}/ 10^5 s^{-1}
1a	1100 ± 200	19.3	+0.162	4.8 ± 0.5	(4.4)[e]
1b	900 ± 150	−4.0	−0.034	*f*	*f*
1c	1900 ± 300	−5.6	−0.119	7.0 ± 0.7	(3.7)[e]
1d	180 ± 20	5.6	+0.069	3.3 ± 0.4	(18)[e]
1e	250 ± 20	−1.9	−0.025	2.6 ± 0.6	(10)[e]
1f	20 ± 10[g]	1.1	+0.045	3 ± 1[h]	120 ± 50[h]

[a] Ground-state binding constants from UV and ^1H NMR. [b] ICD ellipticity at band maximum for 4 mM solutions of **1** (1.0 mM for **1c**) in the presence of β-CD (12.0 mM) in D_2O. [c] Molar ellipticity calculated as $\Delta\epsilon = \theta/(32982\ l\ c)$, cf. ref 76, with l = path length and c = actual concentration of complex in solution calculated by using the binding constants in this table. [d] Association rate constants in the excited state from the time-resolved and steady-state fluorescence quenching data by employing simultaneous fitting according to eqs 6 and 9. [e] Dissociation rate constant estimated as k_{ass}/K. [f] Quenching effect too small to analyze kinetics, cf. text. [g] Determined from ICD titration. [h] Obtained from global fitting to eqs 6 and 7, cf. text.

All azoalkanes **1a**−**f** display exceedingly long fluorescence lifetimes in deaerated D_2O between 730 and 920 ns (Table 1). Table 1 contains also the fluorescence lifetime in the corresponding β-CD·**1** complex (τ_{CD} values), which can be obtained from kinetic measurements in the presence of β-CD (see below). These reflect the reactivity of the excited azoalkane toward abstractable C−H hydrogens in the CD cavity. The method to determine the association rate constants (see below) relies on a fast quenching inside the CD cavity, i.e., small τ_{CD} values. Otherwise, exit from the cavity may compete with deactivation, which complicates the data analysis. The observed trend of the τ_{CD} values, i.e., **1c** ≪ **1a**, **1f** < **1d** < **1e** ≪ **1b**, corresponds to that observed for the solvent-induced quenching by *n*-hexane, cf. lifetimes in this solvent in Table 1: **1c** (30 ns) ≪ **1a** (340 ns) ≈ **1d** (335 ns) < **1e** (420 ns) ≪ **1b** (770 ns). This correlation is reasonable since the same quenching mechanism applies for both *n*-hexane and the interior of β-CD, namely an "aborted" hydrogen abstraction from C−H bonds.[27,39]

Shorter fluorescence lifetimes correspond to higher reactivity for hydrogen abstraction. Accordingly, the chlorinated derivative **1c** is the most reactive one, while the bis-alkylated derivative **1b** displays the lowest reactivity.[40] The hydroxymethyl- and aminomethyl-substituted azoalkanes fall in between. Hence, it appears that electron-withdrawing groups enhance the reactivity of these azoalkanes toward hydrogen donors, while electron-donating groups lower it.[40] This variation can be related to the changes in excitation energy, since the chlorinated derivative exhibits a significantly hypsochromically shifted absorption maximum (Figure 1), corresponding to a higher excitation energy. In addition to variations of the excitation energy, different contributions of charge transfer to the quenching mechanism may apply.[41,42]

Acid−Base Equilibrium of Azoalkanes 1e and 1f. The pK_a value of azoalkane **1e** can be readily determined through measurement of the ^1H NMR chemical shift of the α-CH_2 protons in D_2O ($\delta_{\mathbf{1e}}$ = 3.18 ppm and $\delta_{\mathbf{1f}}$ = 3.62 ppm) as a function of pH. A pK_a value of 9.2 in D_2O was obtained by

(39) Nau, W. M.; Greiner, G.; Wall, J.; Rau, H.; Olivucci, M.; Robb, M. A. *Angew. Chem., Int. Ed.* **1998**, *37*, 98−101.
(40) Zhang, X.; Nau, W. M. *J. Inf. Recording* **2000**, *25*, 323−330.
(41) Pischel, U.; Zhang, X.; Hellrung, B.; Haselbach, E.; Muller, P.-A.; Nau, W. M. *J. Am. Chem. Soc.* **2000**, *122*, 2027−2034.
(42) Sinicropi, A.; Pischel, U.; Basosi, R.; Nau, W. M.; Olivucci, M. *Angew. Chem., Int. Ed.* **2000**, *39*, 4582−4586.

Scheme 1

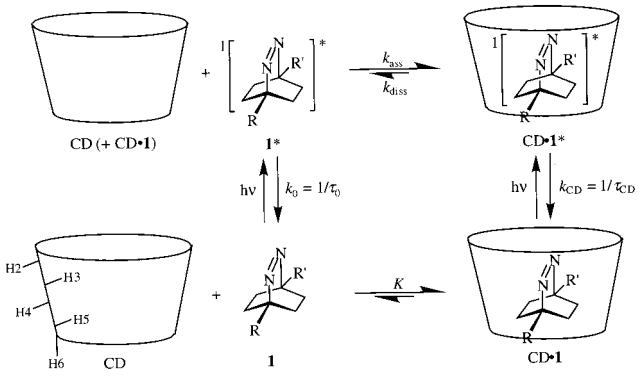

nonlinear least-squares fitting of the chemical shifts according to eq 1.[43] This value falls in the range of those for other amines

$$\delta_{obs} = \frac{\delta_{1e}K_a + \delta_{1f}[H^+]}{K_a + [H^+]} \quad (1)$$

with electron-withdrawing β substituents.[44] Note that the azo group in **1e** can be considered as such an electron-withdrawing β substituent (cf. Hammett σ value of 0.39 for *p*-N=NPh).[45]

Binding Constants. According to Scheme 1, a ground-state equilibrium exists between the free, uncomplexed form (**1**) and the complex (CD•**1**), which is characterized by the binding constant *K* (Table 2). The six differently substituted guest molecules show significant variations of the binding constants, which can be obtained by UV, NMR, ICD, and fluorescence titrations.[26] At least two independent techniques, generally UV and NMR, were employed for each guest, and the results were the same within error. The obtained data confirmed the formation of 1:1 complexes in all cases. For the protonated azoalkane **1f**, the UV and NMR spectral changes were too small to allow a reliable determination of the binding constant by these methods. Here, the more sensitive ICD measurement was employed to derive a much smaller binding constant (20 M^{-1}, see below) than for the amine **1e** (250 M^{-1}).

Induced Circular Dichroism. The analysis of the sign and intensity of the ICD effect arising from the n,π^* transition of azoalkanes has recently been recognized as a powerful tool for structure elucidation of their CD complexes in solution.[29−32] The ICD spectra of all β-CD complexes of azoalkanes **1a**−**f** were measured (Figure 2).[46] The molar ellipticities ($\Delta\epsilon$) were quantified through the respective concentrations and were corrected for the percentage of complexed guest by using the known binding constants (Table 2). For the determination of ICD effects of the amine form **1e** and the ammonium form **1f**, the pH values were again adjusted to 11 and 5. The parent compound **1a** gave a strong, positive ICD signal, and its monosubstituted derivatives **1d** and **1f** showed also a positive, but weaker signal, whereas the disubstituted derivatives **1b** and **1c**, as well the amino derivative **1e**, gave rise to negative ICD effects. Since the ICD signals report selectively on the population of the β-CD complexes, while the uncomplexed components

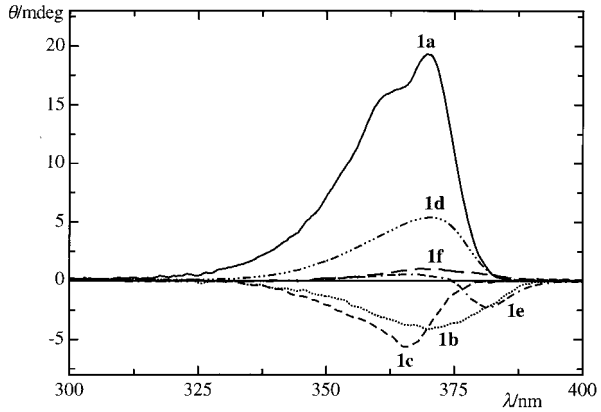

Figure 2. ICD spectra of 4.0 mM solutions (1.0 mM for **1c**) of azoalkane **1a** (—), **1b** (···), **1c** (- - -), **1d** (—···—), **1e** (— —·— —), and **1f** (— — —) in the presence of β-CD (12.0 mM) in D_2O.

Scheme 2

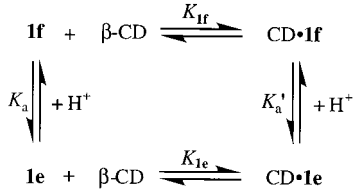

are ICD silent, this titration method may in some cases be more sensitive to determine the binding constants. For **1f**, ICD proved to be the method of choice to determine the binding constant since shifts in the UV and NMR spectra were too small to allow accurate titrations.

Addition of β-CD to a solution of **1e** results in a multiple acid−base equilibrium (Scheme 2),[33,47] and the variation of the ICD spectra with increasing pH reveals an interesting inversion in the sign of the ICD (Figure 3). This can be related to a structural change upon deprotonation (cf. Discussion).

From the thermodynamic cycle in Scheme 2, it is possible to determine the pK_a' value of the β-CD•**1e** complex from eq 2. One obtains a pK_a' value of 8.1, which reveals an apparently

$$K_a' = K_a K_{1e}/K_{1f} \quad (2)$$

lower basicity for the β-CD•**1e** complex compared to the free amine **1e** (pK_a = 9.2). This is synonymous with a higher preference of the ammonium compared to the amine form to remain in the aqueous phase. The known values for the two binding constants (Table 2) and the two pK_a values allow one also to fit the pH profile of the variation of the observed

(43) Arrowsmith, C. H.; Guo, H.; Kresge, A. J. *J. Am. Chem. Soc.* **1994**, *116*, 8890−8894.
(44) Jencks, W. P.; Regenstein, J. In *CRC Handbook of Biochemistry and Molecular Biology*, 2nd ed.; Sober, H. A., Ed.; CRC Press: Cleveland, OH, 1970; pp J187−J226.
(45) Hansch, C.; Leo, A.; Taft, R. W. *Chem. Rev.* **1991**, *91*, 165−195.

(46) ICD spectra were also obtained for azoalkanes **1** in the presence of α-CD and γ-CD as inducers. The experimental ICD intensities (θ/mdeg) at the band maximum of 4 mM solutions of azoalkanes **1** (1.0 mM for **1c**) in the presence of α-CD (12.0 mM) in D_2O were as follows: +14 for **1a**, +0.5 for **1b**, 0 for **1c**, and +0.5 for **1d**. In the presence of γ-CD (12.0 mM) the intensities were +1.5 for **1a**, +8.0 for **1b**, +2.1 for **1c**, and +2.5 for **1d**. As can be seen, the ICD signals were consistently positive, but for **1b**−**d** in the presence of α-CD, hardly any effect was noticed, which paralleled the absence of a significant effect on the UV spectra in these cases. The binding constants for α-CD and γ-CD are generally much lower than those for β-CD; e.g., for α-CD•**1a** ca. 50 M^{-1}, for β-CD•**1a** 1100 M^{-1}, for γ-CD•**1a** ca. 6 M^{-1} (ref 26); for α-CD•**1b** <3 M^{-1}, for β-CD•**1b** 900 M^{-1}, and for γ-CD•**1b** 150 M^{-1} (this work). More detailed investigations with the other cyclodextrins were not undertaken, since the weaker binding imposes experimental complications. Moreover, α-CD appears to be too small to form deep inclusion complexes with the guests, cf. absence of binding for **1b**−**d**, while γ-CD may be too large to cause a clear preference for a particular co-conformation.
(47) Yoshida, N.; Seiyama, A.; Fujimoto, M. *J. Phys. Chem.* **1990**, *94*, 4254−4259.

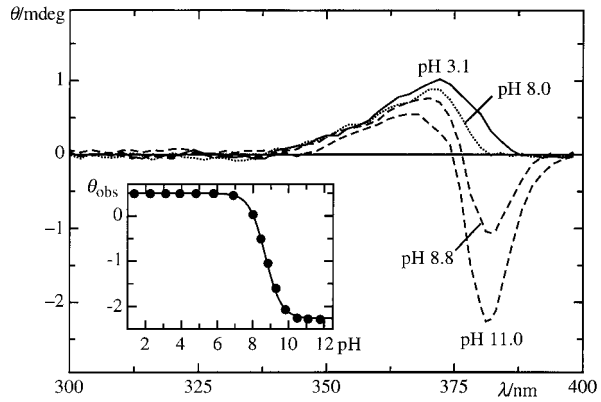

Figure 3. ICD spectra for azoalkane **1e** (4.0 mM) in the presence of β-CD (12.0 mM) in D_2O at varying pH values. The inset shows a plot of the ellipticity at 381 nm versus pH fitted according to eq 3.

ellipticity (θ_{obs}), e.g., in the region of maximum variation at 381 nm.[48] We have derived eq 3 to describe the pH dependence of the ellipticity (l = path length). The resulting fit[49] (inset in Figure 3) corroborates the applicability of Scheme 2. It should be noted that the analytical form of eq 3 should be generally applicable to describe related pH effects on ICD spectra.

$$\frac{\theta_{obs}}{32982\,l} = \Delta\epsilon_{\mathbf{1e}}[\mathrm{CD}\cdot\mathbf{1e}] + \Delta\epsilon_{\mathbf{1f}}[\mathrm{CD}\cdot\mathbf{1f}]$$

$$= \Delta\epsilon_{\mathbf{1e}}PK_a' + \Delta\epsilon_{\mathbf{1f}}P[H^+] \qquad (3)$$

$$\text{with} \quad P = \frac{[\mathbf{1e}]_0 + [\mathrm{CD}]_0}{2(K_a' + [H^+])} + \frac{K_a'([H^+] + K_a)}{2K_{\mathbf{1e}}K_a(K_a' + [H^+])^2} -$$

$$\{(K_{\mathbf{1e}}K_a([\mathbf{1e}]_0 + [\mathrm{CD}]_0)(K_a' + [H^+]) + K_a'([H^+] + K_a))^2 -$$
$$4[\mathbf{1e}]_0[\mathrm{CD}]_0K_{\mathbf{1e}}{}^2K_a{}^2(K_a' + H^+])^2\}^{1/2}/2K_{\mathbf{1e}}K_a(K_a' + [H^+])^2$$

The maxima of the ICD bands matched the UV absorption maxima for all β-CD·**1** complexes except for **1b** and **1e**. A hypsochromic shift from 379 nm (UV) to 370 nm (ICD) was registered for **1b** and a bathochromic shift from 373 nm (UV) to 382 nm (ICD) for **1e**. The ICD spectrum for **1e** exhibited also a distorted band shape, cf. pH 11 spectrum in Figure 2. These shifts may be indicative of a large co-conformational variability or nonuniformity (cf. Discussion).

Association Rate Constants. It should be noted in advance that our kinetic interpretations of the kinetic parameters are based on Scheme 1, which has been demonstrated to hold for the parent compound **1a**.[26] Excitation by UV light around 370 nm populates the fluorescent singlet-excited state of the free azoalkane (**1***) and the complex (CD·**1***). The environmental dependence of the fluorescence of **1** (quenching by abstractable C-H bonds) results in a shorter fluorescence lifetime within the complex (τ_{CD}) compared to the uncomplexed form (τ_0), see above. The kinetics can be analyzed through steady-state fluorescence measurements, which rely on the concomitant decrease of integrated fluorescence intensity upon addition of CD. These measurements require excitation at the isosbestic point (λ_{iso}, Table 1).[26] The intensity ratio in the absence (I_0)

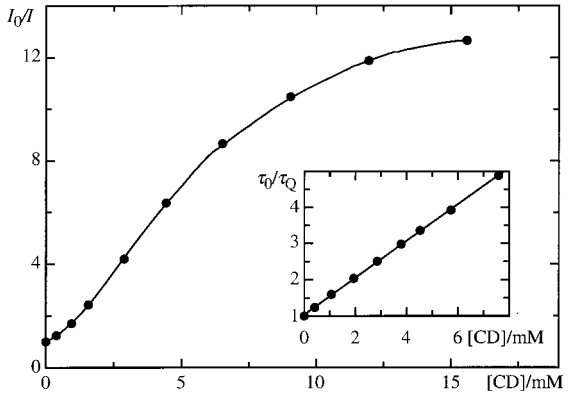

Figure 4. Steady-state and kinetic (inset) fluorescence quenching plots for **1c** (1.0 mM) by β-CD in D_2O and fits according to eqs 6 and 9 and the parameters in Table 2 (solid lines).

and in the presence of CD (I) is plotted against the total concentration of CD ($[CD]_0$) according to the previously introduced[26] eq 4, in which the concentration of uncomplexed azoalkane, [**1**], is defined by eq 5. Because the lifetime of the uncomplexed form (τ_0 in eq 4) and the binding constants (K in eq 5, Table 2) are known otherwise (Table 1), such plots (see Figure 4) are suitable to provide values for the association rate constant (k_{ass}), the dissociation rate constant (k_{diss}), and the fluorescence lifetime of the complex (τ_{CD}). τ_Q in eq 4 is the lifetime of the free excited guest, i.e., before it either deactivates or complexes with β-CD.

$$\frac{I}{I_0} = \frac{[\mathbf{1}]}{[\mathbf{1}]_0}\frac{\tau_Q}{\tau_0} + \frac{[\mathbf{1}]}{[\mathbf{1}]_0}QR\frac{\tau_{CD}}{\tau_0} + \left(1 - \frac{[\mathbf{1}]}{[\mathbf{1}]_0}\right)R\frac{\tau_{CD}}{\tau_0} \qquad (4)$$

$$\text{with} \quad Q = \frac{k_{ass}\tau_0[\mathrm{CD}]_0}{1 + k_{ass}\tau_0[\mathrm{CD}]_0},$$

$$R = \frac{1 + k_{ass}\tau_0[\mathrm{CD}]_0 + k_{diss}\tau_0}{1 + k_{ass}\tau_0[\mathrm{CD}]_0 + k_{diss}\tau_{CD}}, \text{ and } \tau_Q = \frac{1}{k_0 + k_{ass}[\mathrm{CD}]_0}$$

$$[\mathbf{1}] = (K[\mathbf{1}]_0 - K[\mathrm{CD}]_0 - 1 + \{(K[\mathbf{1}]_0 + K[\mathrm{CD}]_0 + 1)^2 -$$
$$4K^2[\mathbf{1}]_0[\mathrm{CD}]_0\}^{1/2})/2K \qquad (5)$$

The k_{diss} values recovered from fits according to eq 4 were very small for azoalkanes **1a**−**e**, and the errors were as large as the values themselves. This result confirmed that exit from the excited complex must be indeed insignificant for azoalkanes **1a**−**e**, as previously demonstrated for **1a**.[26] This was not the case for the ammonium derivative **1f**, for which the value of k_{diss}, within a large error, was only 1 order of magnitude below that of k_{ass}. This indicated the significance of exit in this case. If one assumes that the binding constants are similar in the ground and excited states (see Discussion), one may obtain estimates of the dissociation rate constants (k_{diss}, values in parentheses in Table 2). These values are much smaller than $k_{CD} = 1/\tau_{CD}$, the quenching rate constant inside the complex, *except for* **1f**. This supports the notion that k_{diss} cannot be neglected for **1f**, but it can be for the other derivatives **1a**−**e**, for which the simplified eq 6 can then be applied for fitting and extracting the values of k_{ass}.

$$\frac{I}{I_0} = \frac{\tau_{CD}}{\tau_0} + \frac{[\mathbf{1}]}{[\mathbf{1}]_0}\left(1 - \frac{\tau_{CD}}{\tau_0}\right)\left(\frac{1}{1 + k_{ass}\tau_0[\mathrm{CD}]_0}\right), \quad \text{for } k_{diss} \ll k_{CD} \qquad (6)$$

(48) Yi, Z.; Chen, H.; Huang, Z.; Huang, Q.; Yu, J. *J. Chem. Soc., Perkin Trans. 2* **2000**, 121−127.
(49) The computer program Pro Fit 5.5.0 (QuantumSoft, Zurich) was employed for individual fitting and global data analysis.

The time-resolved fluorescence decays were obtained by laser-flash photolysis. The resulting kinetics can be analyzed according to the formal kinetic scheme derived by Andriessen et al.[50] In our fluorescence measurement, both the free fluorophores and the complexes are simultaneously excited due to the very similar UV absorption spectra. Moreover, since the fluorescence spectra are virtually superimposable,[26,27] the sum of the fluorescence from both species is observed. If one further ensures equal absorption probabilities by excitation at the isosbestic point (λ_{iso}, Table 1) or corrects for differential absorption in cases where the excitation wavelength cannot be adjusted (e.g., for laser excitation), and in addition relies on the observation that the natural radiative lifetimes display no pronounced solvent dependence,[27] the emission intensities of each species are linearly related to its ground-state concentration. The time dependence of the observed fluorescence intensity, $I(t)$, normalized to unity at $t = 0$, is then given by eq 7, where [**1**] is defined by eq 5.

$$I(t) = \left(\frac{-[\mathbf{1}](k_0+\gamma_2) - [\mathrm{CD}\cdot\mathbf{1}](k_{CD}+\gamma_2)}{[\mathbf{1}]_0\sqrt{(k_0+k_{ass}[CD]_0-k_{CD}-k_{diss})^2+4k_{ass}k_{diss}[CD]_0}}\right)e^{\gamma_1 t} + \left(\frac{[\mathbf{1}](k_0+\gamma_1) + [\mathrm{CD}\cdot\mathbf{1}](k_{CD}+\gamma_1)}{[\mathbf{1}]_0\sqrt{(k_0+k_{ass}[CD]_0-k_{CD}-k_{diss})^2+4k_{ass}k_{diss}[CD]_0}}\right)e^{\gamma_2 t} \quad (7)$$

The time constants γ_1 and γ_2 in eq 7 are defined as follows:

$$\gamma_1 = -\frac{1}{2}\{k_0 + k_{ass}[CD]_0 + k_{CD} + k_{diss} - \sqrt{(k_0+k_{ass}[CD]_0-k_{CD}-k_{diss})^2+4k_{ass}k_{diss}[CD]_0}\}$$

$$\gamma_2 = -\frac{1}{2}\{k_0 + k_{ass}[CD]_0 + k_{CD} + k_{diss} + \sqrt{(k_0+k_{ass}[CD]_0-k_{CD}-k_{diss})^2+4k_{ass}k_{diss}[CD]_0}\}$$

When dissociation of the complex during its excited-state lifetime is negligible ($k_{diss} \ll k_{CD}$), eq 7 simplifies to the equation employed in our previous work (here rearranged):

$$I(t) = (1-S)\,e^{-(\tau_{CD})^{-1}t} + S\,e^{-(\tau_Q)^{-1}t}$$

$$\text{with} \quad S = \frac{[\mathbf{1}]}{[\mathbf{1}]_0}\left(1 + \frac{k_{ass}\tau_0[CD]_0}{\tau_0/\tau_{CD} - k_{ass}\tau_0[CD]_0 - 1}\right) \quad (8)$$

$$\text{and} \quad \tau_Q = \frac{1}{k_0 + k_{ass}[CD]_0}, \text{ for } k_{diss} \ll k_{CD}$$

An analysis of the preexponential factors in eqs 7 and 8, which are subject to a larger error,[26] was generally not attempted, but the two time constants (τ_{CD} and τ_Q) in the experimental decay traces were extracted by biexponential fitting. For azoalkanes **1a**−**e**, one component was found to be *constant* within error, i.e., independent of CD concentration. This suggested that eq 8 applied, in which exit is considered insignificant for **1a**−**e**, as already borne out by the steady-state analysis above. The meaning of the time constants in eq 8 can be readily rationalized. The first time constant corresponds to a *static* component (τ_{CD}), which is due to quenching inside the complex (Scheme 1) and therefore independent of CD concentration. The second, *dynamic* component (τ_Q) corresponds to the lifetime of the free form before complexation, which depends on the bimolecular association rate constant (k_{ass}) and the CD concentration. k_{ass} can then be extracted from the dependence of the τ_Q values on the total CD concentration (eq 9). Here, the analysis according to eq 8 rather than eq 7 has the advantage of a simple linearized data representation (eq 9) through a regression analysis of a kinetic quenching plot (inset in Figure 4).

$$\frac{\tau_0}{\tau_Q} = 1 + k_{ass}\tau_0[CD]_0 \quad (9)$$

In a final procedure, to obtain the best estimates of the association rate constants for azoalkanes **1a-e**, where exit is insignificant, the time-resolved and steady-state data were subjected to a *simultaneous* nonlinear fitting analysis according to eqs 6 and 9, putting arbitrarily an equal weight to both data sets.[49] The resulting values are entered in Table 2. For the ammonium derivative **1f**, the biexponential fitting of the excited-state lifetimes did not yield a static, i.e., constant, component at different CD concentrations. This, along with the indications from the steady-state experiments (see above), suggested that exit cannot be neglected and that eqs 6 and 9 no longer apply. This prevented also an analysis of the time-resolved data according to eq 9. A global analysis,[49] i.e., simultaneous fitting of the individual decay traces according to eq 7, is indicated in such cases,[50] which includes k_{diss} as a fitting parameter. Moreover, we have also included the steady-state treatment according to eq 4, which considers also k_{diss}, in the final analysis, putting again an equal weight to the steady-state and the combined time-resolved data. The resulting constants for **1f** are entered in Table 2. It should be mentioned that the binding constant obtained from the ratio of the recovered rate constants ($k_{ass}/k_{diss} = 25\ M^{-1}$) supports also the suggestion that the excited-state binding resembles that in the ground state (20 M^{-1}), which was obtained by ICD (see above).

For azoalkane **1b**, for which the fluorescence lifetime of the complex (τ_{CD}) was very long (430 ns) and too similar to that of the uncomplexed guest (590 ns, under air), a reliable differentiation of the static and dynamic components through biexponential fitting of the time-resolved decay traces could not be performed. In general, the differentiation of two exponential decay components becomes a formidable task when the lifetimes differ by less than a factor of 2.[51] The effects on the steady-state fluorescence intensity were also too small in relation to the error to allow a reliable fitting according to eq 6. As a consequence, no kinetic data for **1b** can be reported. The failure for **1b** reveals the limitations of our fluorescence-based method for determining association rate constants.

Discussion

The changes of the UV, ICD, and NMR spectra of azoalkanes **1** upon addition of β-cyclodextrin (β-CD) can be understood in terms of the formation of inclusion complexes, where the guest is positioned inside a hydrophobic cavity. This is confirmed,

(50) Andriessen, R.; Boens, N.; Ameloot, M.; De Schryver, F. C. *J. Phys. Chem.* **1991**, *95*, 2047−2058.

(51) Grinvald, A.; Steinberg, I. Z. *Anal. Biochem.* **1974**, *59*, 583−598.

for example, by the bathochromic shift of the near-UV azo absorption band (Table 1) and the chemically induced ^{1}H NMR shifts (CIS), which were observed for the inner H-3 and H-5, yet not for the outer H-2 and H-4 protons of β-CD (the approximate locations of these hydrogens are entered in Scheme 1, bottom left). The CIS values are significant not only for the upper H-3 (ca. 0.10 ppm) but also for the lower H-5 protons (ca. 0.08 ppm). This applies for all azoalkanes **1a**−**f** when the effects are extrapolated to quantitative binding. A small effect was also observed for the H-6 protons. The observed NMR shifts can be conclusively interpreted in terms of a *deep* inclusion for all complexes, as previously corroborated for azoalkanes **1a** and **1b**.[26,29] All data support the formation of complexes with 1:1 stoichiometry; e.g., the UV titrations show an isobestic point (Table 1) and the data from UV, NMR, fluorescence, and ICD titrations can be fitted with a 1:1 complexation model.

The Discussion is arranged such that we will first analyze the structure of the host−guest complexes in more detail, in particular with respect to the relative alignment of the guest to the host, i.e., the co-conformation of the complex.[12] In a second part, substituent effects on the thermodynamics of binding will be examined, keeping in mind a possible influence of structural variations. Finally, we will question to which degree the kinetics of host−guest complex formation can be understood in terms of the observed structural and thermodynamic trends.

Complex Structures by Induced Circular Dichroism and NMR. The induced circular dichroism (ICD) provides a unique analytical tool to investigate the structures of chiral host−guest (host−chromophore) inclusion complexes in solution.[6,7,11] Several rules for the assignment of the co-conformations and the depth of inclusion have been developed for cyclodextrins (CDs) as host systems.[10,52,53] In most studies, aromatic chromophores have been examined, whereas aliphatic ones have received comparably little attention. Aliphatic azoalkanes and diazirines have recently been employed in ICD measurements,[29−32] which has allowed several new insights into the inclusion geometries of aliphatic guests.

The ICD method was also applied in this work to the complexes between β-CD as chiral host and azoalkanes **1** as achiral chromophores.[46] In essence, the n,π* transition of the azo chromophore around 370 nm gives rise to a characteristic ICD signal when included in CD.[29−32] The magnitude and sign of the ICD effect are directly related to the orientation of the electric dipole transition moment relative to the axis of the CD. According to the rule of Harata,[10,29,30,53] which applies to chromophores immersed in the CD cavity, co-conformations with a parallel alignment produce a positive ICD signal, while those with an orthogonal alignment produce only a half as strong, negative ICD signal. In the case of azoalkanes, the electric dipole transition moment points along the azo π orbital and lies orthogonal to the plane defined by the C−N═N−C linkage.[29] Structural assignments of the β-CD complexes of the parent compound **1a** and the bis-alkylated derivative **1b** based on ICD effects have been communicated (Scheme 3, arrows indicate the direction of the electric dipole transition moment).[29] We refer to the respective co-conformations as lateral (**1a**) and frontal (**1b**).[29] These assignments have been recently confirmed

Scheme 3

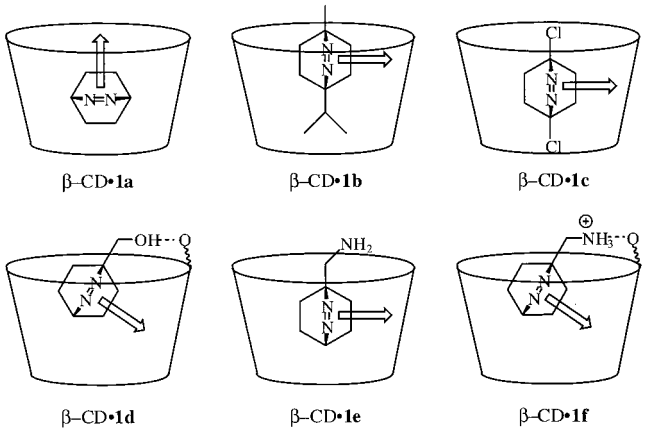

through force-field computed structures and energies as well as quantum-chemical calculations of ICD effects.[30]

The co-conformational assignments of the presently examined derivatives **1c**−**e** are made accordingly (Scheme 3), keeping in mind the NMR results (see above) which suggest the formation of deep inclusion complexes in all cases. Further, we adhere to the general notion that polar substituents reside near the secondary hydroxyl rim while more hydrophobic groups tend to protrude into the cavity.[6] For **1b**, in particular, the penetration of the isopropyl rather than the methyl group has been substantiated by force-field calculations.[30] The dichloro derivative **1c** resembles the bis-alkylated derivative **1b** in that it bears two bridgehead substituents. The van der Waals diameters along the bridgehead axis of **1c** (ca. 8 Å) and **1b** (ca. 9 Å) both exceed the diameter of the β-CD cavity (6.0−6.5 Å)[1] significantly, which promotes a frontal type of inclusion due to steric restraints.[29] The strong negative ICD for **1c** supports this structural assignment (Scheme 3).

The van der Waals diameter of the hydroxymethyl, aminomethyl, and ammoniummethyl derivatives **1d**−**f** (ca. 7 Å along bridgehead axis) lies between those for the parent **1a** (ca. 6 Å) and the disubstituted cases **1b** and **1c**. This reduces the preference for frontal inclusion, but a lateral or tilted lateral inclusion may still be viable. Indeed, the hydroxy and ammonium derivatives **1d** and **1f** display positive ICD effects, which suggest a more lateral co-conformation, as has been previously observed and analyzed for the parent compound **1a**. Note that among the four principal co-conformations (lateral, frontal, apical, basal), only the lateral one should give rise to a positive ICD.[29,30] Due to the angular dependence of the ICD effect in CD inclusion complexes, which predicts positive contributions to be twice as strong as negative ones for the same electronic transition,[10,29,30,53] a positive ICD signal is expected even for significant deviations from the ideal angle (Harata's rule, see above).[30]

Strikingly, the aminomethyl derivative produced a negative ICD effect, which resembles that observed for the bis-substituted derivatives **1b** and **1c**. This suggests that a frontal co-conformation is populated for **1e**. But why does the substitution of the hydroxy for the amino group (**1d** versus **1e**) or even the deprotonation of the ammonium group (**1f** versus **1e**) result in an inversion of the ICD sign from positive to negative, i.e., a pronounced change in the co-conformation of the host−guest complex? We propose that differences in host−guest hydrogen bonding are important. The intramolecular network of secondary

(52) Kajtár, M.; Horváth-Toró, C.; Kuthi, É.; Szejtli, J. *Acta Chim. Acad. Sci. Hung.* **1982**, *110*, 327−355.
(53) Kodaka, M. *J. Phys. Chem. A* **1998**, *102*, 8101−8103.

Scheme 4

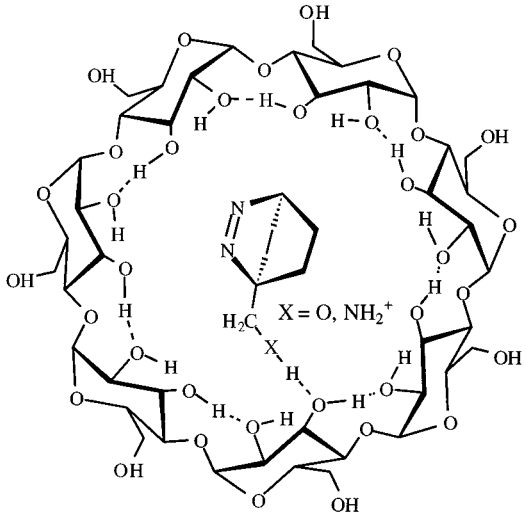

O2(n)···H···O3(n − 1) interglucose hydrogen bonds[9,54,55] stabilizes the macrocyclic host structures. These intramolecular hydrogen bonds at the upper rim are particularly strong for β-CD[56] compared to α-CD and γ-CD, which is also held responsible for the reduced solubility of β-CD.[57] It is conceivable that the intramolecular network prefers intermolecular interactions with hydrogen bond *donors* over those with hydrogen bond *acceptors* (Scheme 4). In fact, in most documented cases for hydrogen bonding, the guests, in particular phenols,[7,58−60] function as hydrogen bond donors.

The tendency for formation of hydrogen bonds in which the functional groups act as donors should approximately decrease with the group acidity, which follows the well-known order $R-NH_3^+ > R-OH \gg R-NH_2$. The hydroxyl and ammonium groups in **1d** and **1f** may thus form hydrogen bonds with the secondary hydroxyl rim (Scheme 4)[48,61] and, thus, adapt a tilted lateral co-conformation (Scheme 3). In contrast, the amino group as the poorest hydrogen bond donor may not form such hydrogen bonds. Steric effects (as those for **1b** and **1c**) may now prevail and induce a frontal co-conformation with the expected negative ICD. Hence, the variations in the signs of the experimental ICD effects may be due to a change of the co-conformations of azoalkanes **1d**−**f** as induced by hydrogen bonding with the secondary hydroxyl rim for the hydroxyl and ammonium but not for the amino group.

These tentative structural assignments are in line with literature findings. First, a lower tendency for hydrogen bonding of the amino compared to the hydroxyl group has been previously held responsible for a similar structural effect, namely a more axial co-conformation of anilines compared to phenols.[58] Second, according to crystal structures, the amino group in *p*-iodoaniline in its α-CD complex adapts a position very similar

Scheme 5

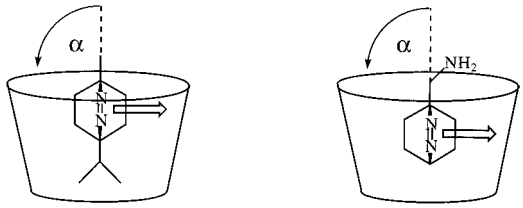

to that depicted in Scheme 3 for **1e** and does not engage in hydrogen bonding with the enclosing host, either.[62]

Based on the relative magnitude of the ^{1}H NMR shifts, H-3 > H-5 ≫ H-6, we propose for all azoalkanes **1a**−**f** a location with the center of mass somewhat displaced toward the upper rim, as previously found for **1b** by force-field calculations.[30] This location renders also hydrogen bonding of the functional groups in **1d** and **1f** with the lower rim O-6 protons unlikely, i.e., a 180° rotation of these guest molecules in Scheme 3. Such alternative hydrogen bonding with the primary hydroxyl rim has been occasionally invoked for very small guest molecules.[62] However, bonding with the upper secondary hydroxyl rim as depicted for **1d** and **1f** in Scheme 3 is more common.[48,60,61,63−66]

While we assume that the structure of the β-CD•**1e** complex in Scheme 3 gives rise to the negative ICD signal, scrutiny of the ICD spectra reveals that the complex of azoalkane **1e** differs from the other derivatives in that it gives rise to an ICD band, which is significantly distorted, cf. Figure 2, and shows also a bathochromic shift relative to the UV spectrum (cf. Results). A small shift of the band maximum of the UV and ICD spectrum was also observed for azoalkane **1b**, but not for the other four derivatives, for which the band shape and maximum were virtually the same. Moreover, the ICD of **1e** shows a small positive component at shorter wavelengths in addition to the stronger negative one. These irregularities suggest a large co-conformational variability, which has been previously corroborated for **1b**.[30] This means that complexes with different tilt angles (α in Scheme 5) may be present in solution. Note, in particular, that for **1e**, in contrast to **1d** and **1f**, the co-conformational space may not be restricted by hydrogen bonding with the upper rim. The co-conformers with different tilt angles may have quite different UV spectra (which reflect the depth of inclusion into the nonpolar environment) and ICD effects (which reflect the geometrical alignment with respect to the azo chromophore) and, thus, account for the observed shifts for **1b** and **1e**. For example, a tilted, less deeply immersed complex could be responsible for the small positive ICD contributions for **1e** at short wavelengths.

The possible involvement of more than one co-conformer and a large co-conformational variability constitute standing problems in the assignment of the solution structures of host−guest complexes. This is in contrast to crystal structures where one co-conformer may crystallize out preferentially, which does not

(54) Jacob, J.; Gessler, K.; Hoffmann, D.; Sanbe, H.; Koizumi, K.; Smith, S. M.; Takaha, T.; Saenger, W. *Angew. Chem., Int. Ed.* **1998**, *37*, 605−609.
(55) Harata, K. *Bull. Chem. Soc. Jpn.* **1982**, *55*, 2315−2320.
(56) Steiner, T.; Saenger, W. *Angew. Chem., Int. Ed.* **1998**, *37*, 3404−3407.
(57) Szejtli, J. *Cyclodextrin Technology*; Kluwer: Dordrecht, 1988.
(58) Kamiya, M.; Mitsuhashi, S.; Makino, M.; Yoshioka, H. *J. Phys. Chem.* **1992**, *96*, 95−99.
(59) Rekharsky, M. V.; Goldberg, R. N.; Schwarz, F. P.; Tewari, Y. B.; Ross, P. D.; Yamashoji, Y.; Inoue, Y. *J. Am. Chem. Soc.* **1995**, *117*, 8830−8840.
(60) Marconi, G.; Monti, S.; Mayer, B.; Köhler, G. *J. Phys. Chem.* **1995**, *99*, 3943−3950.
(61) Roberts, E. L.; Dey, J.; Warner, I. M. *J. Phys. Chem. A* **1997**, *101*, 5296−5301.
(62) Saenger, W.; Beyer, K.; Manor, P. C. *Acta Crystallogr.* **1976**, *B32*, 120−128.
(63) Wenz, G.; Hoefler, T.; Wehrle, S.; Schneider, M. *Polym. Prepr. (Am. Chem. Soc., Div. Polym. Chem.)* **1998**, *39*, 202−203.
(64) Kano, K.; Tatsumi, M.; Hashimoto, S. *J. Org. Chem.* **1991**, *56*, 6579−6585.
(65) Amato, M. E.; Djedaini-Pilard, F.; Perly, B.; Scarlata, G. *J. Chem. Soc., Perkin Trans. 2* **1992**, 2065−2069.
(66) Krishnamoorthy, G.; Dogra, S. K. *J. Phys. Chem. A* **2000**, *104*, 2542−2551.

necessarily provide evidence for the prevalence of this particular co-conformer in solution. The possibility of several populated co-conformers exposes also the limitations of ICD spectra for structural assignments, since ICD spectra reflect a Boltzmann-weighted average of all thermally accessible structures. In general, one must note that the proposed structural assignments based on NMR and ICD effects (Scheme 3) are tentative ones, since they rely, for example, on empirical rules for the interpretation of ICD effect. However, one must also recall that the determination of the solution structures of cyclodextrin complexes by NMR and ICD presents a great challenge since alternative experimental methods have not been established.

The *absolute* magnitude of the ICD effects can be compared on the basis of the molar ellipticity values ($\Delta\epsilon$, Table 2), which extrapolate the experimental θ values to quantitative complexation and, thus, present a comparable quantity for all complexes. The order observed for the positive ICD effects, i.e., **1a** > **1d** ≈ **1f**, is in agreement with the suggestion that **1d** and **1f** adapt a similar co-conformation, which, however, is somewhat less ideal than for azoalkane **1a**, i.e., the lateral co-conformation which gives rise to the positive ICD is somewhat tilted. The order observed for the negative ICD effects, i.e., **1c** < **1e** ≈ **1b**, suggests that the dichloro derivative **1c** adapts the "most perfect" frontal co-conformation, which may be caused by a particularly strong binding and deep penetration of this derivative into the cavity (see below). For comparison, **1b** may not protrude as deeply due to steric repulsion of the isopropyl group caused by the lower, tighter rim (note the conical shape of CD). This leaves the center of mass of **1b** more displaced toward the upper rim and may also be the reason for the large co-conformational variability, which is indicated for **1b**, yet not for **1c** (see above).[30]

Binding Constants. Relatively few thermodynamic studies of substituent effects have been devoted to aliphatic guest molecules[33,34] as opposed to aromatic guests.[6,7,67] The binding constants in Table 2 for azoalkanes **1** reflect the differential stabilization of the various guest molecules in the bulk water and the CD cavity. This results from a complex interplay between van der Waals and hydrophobic interactions, hydrogen bonding, release of high-energy water from the CD cavity, and relief of CD strain energy.[6,33,67] A quantitative analysis of the trends of the binding constants of azoalkanes **1** (Table 2) is not attempted, but some peculiarities and clear-cut rationalizations are addressed.

The parent compound **1a** serves as a reference with a binding constant of about 1000 M^{-1}. Based on the lower solubility of the dichloro derivative **1c** in water (1.0 mM) compared to the other azoalkanes (>10 mM) and well-known solubility trends (e.g., higher water solubility of alcohols compared to homologous amines), the hydrophobicity order of the examined guest molecules can be established as **1c** > **1b** > **1a** > **1e** > **1d** > **1f**. A higher hydrophobicity is expected to result in a larger binding constant, which is in an overall agreement with the experimental findings (1900 M^{-1} for **1c** > 1000 M^{-1} for **1a**,**1b** > 250 M^{-1} for **1e** > 180 M^{-1} for **1d** > 20 M^{-1} for **1f**). Interestingly, azoalkane **1b** does not show a higher binding affinity than **1a** despite its higher hydrophobicity. This can be rationalized in terms of the solution structures, which indicate that the lateral co-conformation, which is the energetically most favorable one for **1a**,[30] cannot be attained for **1b**. Instead, a frontal mode of inclusion must be adapted (Scheme 3). This co-conformation is energetically less favorable, which may offset the increased driving force due to its higher hydrophobicity and results in essentially the same binding constant as for **1a**.

Generally, the more hydrophilic guests **1d**−**f** show lower binding constants than **1a**−**c**. The ionic ammonium guest **1f** displays the weakest binding. The difference in binding constants between **1e** (250 M^{-1}) and **1f** (20 M^{-1}) is in line with the general observation that the ionization of the guest causes a destabilization of CD complexes in water.[33,68,69] We have shown above that hydrogen bonding is presumably an important structure-determining factor. However, the postulated hydrogen bonding of the hydroxyl and ammonium groups with the hydroxyl rim of the CD is not sufficiently large to result in an increased binding constant compared to that of **1a**. Moreover, the hydroxyl and ammonium derivatives **1d** and **1f**, for which hydrogen bonding is presumed, show actually a weaker binding than the amino derivative, for which hydrogen bonding to the CD may not play a role at all. The absence of a significant thermodynamic stabilization due to hydrogen bonding is in agreement with the results of other authors.[6,7] Consequently, the thermodynamics for binding of azoalkanes **1** is dominated by other factors. Namely, it can be adequately accounted for in terms of guest hydrophobicity and a change in the co-conformation due to the introduction of bridgehead substituents.

Complexation Kinetics. Knowledge of the association and dissociation rate constants of guest molecules with CDs is restricted to case studies,[19−23] and structural effects have only recently received attention.[70] Substituent effects have apparently not been examined for a common guest structure. This challenging aspect can now be studied by using the substituted azoalkanes **1** as dynamic fluorescent probes. As noted in the outset, the fluorescence quenching in the β-CD cavity allows one to obtain the association rate constants, while other techniques have proven particularly suitable for determining dissociation rate constants.[22,23] Strictly speaking, the association rate constants refer to the excited state, but it is presumed that these are comparable with those in the ground state, since the structure of these rigid bicyclic molecules and their dipole moments remain virtually unaffected by the electronic excitation (e.g., 3.5 D in the ground state vs 3.2 D in the singlet-excited state of **1a**).[71] This is in contrast to other guest molecules such as ketones, which undergo large dipole moment changes upon excitation.[22,23] Moreover, the very low pK_a values of the azo group in the ground state (0.5) and excited state (ca. −8) exclude the possibility of differential stabilization due to protonation.[72] In any case, the substituents hardly interact with the azo chromophore (cf. very similar UV spectra), such that the *relative* effects on the association rate constants, i.e., the substituent effects, should be meaningful even if small changes in the absolute thermodynamics due to excitation of the azo group apply.

As can be seen from Table 2, the overall variation in the association rate constants covers only a factor of 2−3, much

(67) Liu, L.; Guo, Q. *J. Phys. Chem. B* **1999**, *103*, 3461−3467.
(68) Matsuura, N.; Takenaka, S.; Tokura, N. *J. Chem. Soc., Perkin Trans. 2* **1977**, 1419−1421.
(69) Bergeron, R. J.; Channing, M. A.; McGovern, K. A. *J. Am. Chem. Soc.* **1978**, *100*, 2878−2883.
(70) Christoff, M.; Okano, L. T.; Bohne, C. *J. Photochem. Photobiol. A: Chem.* **2000**, *134*, 169−176.
(71) Nau, W. M.; Pischel, U. *Angew. Chem., Int. Ed.* **1999**, *38*, 2885−2888.
(72) Nau, W. M. *EPA Newsl.* **2000**, *70*, 6−29.

less than that for the binding constants. Efficient quenching upon complexation is a prerequisite for determining association rate constants by the fluorescence-based method. This is not met for azoalkane **1b**, such that this derivative could not be included in the kinetic analysis. Until recently, most reported association rate constants of small organic guest molecules with β-CD fell in the range of $(4-5) \times 10^8$ M^{-1} s^{-1} or below.[26] Recent measurements suggest that this does not constitute an upper limit and that rate constants may exceed this value.[22,70] The value measured for azoalkane **1c** (7.0×10^8 M^{-1} s^{-1}) is in line with this observation. Since the value for the dichloro derivative **1c** is the largest, a steric effect, which would predict a slower association rate, is clearly not observed. Moreover, the presence of hydrophilic substituents such as hydroxy, amino, and ammonium has no large effect on the kinetics. Consequently, guest desolvation does not dominate the complexation kinetics as in other cases, e.g., in the complexation of cations by crown ethers.[13] Rather, the observed order of the available association rate constants, namely, **1c** > **1a** > **1d**−**f**, follows roughly the order of the binding constants but does not allow definitive conclusions. However, it should be noted that a correlation between the kinetics of complexation and the binding constants is not a priori expected, and contrasting trends were observed in some cases.[73] This circumstance emphasizes the need for measurement of rate constants in addition to binding constants.

The dissociation rate constants (k_{diss}) define the lifetimes of the guests in the CD cavity ($\tau_{diss} = 1/k_{diss}$) and may be directly related to the efficiency of drug delivery and chemical protection of guests.[17,19] These values cannot be directly measured with our method, but they can be calculated from the experimental binding constants (K) and excited-state association rate constants (k_{ass}) subject to the above assumption that photochemical excitation does not significantly modify the affinity for binding. The calculated values for k_{diss} range from 10^5 to 10^7 s^{-1} and are included in Table 2. For **1a**−**e**, these values lie far below the rate constants for fluorescence in the CD cavity ($k_{CD} = 1/\tau_{CD} \approx 1 \times 10^7$ s^{-1}), but for **1f** exit occurs with a similar rate constant. This quantifies the previous notion (expressed for **1a**) that exit from the cavity does not compete significantly with deactivation for **1a**−**e**. Only for **1f** does exit become significant, such that the kinetics required a more evolved analysis in this case (cf. Results).

As previously emphasized, structural effects manifest themselves much more strongly in the exit than in the entry rate constants.[70] This notion is supported for the substituent effects on the dissociation rate constants for azoalkanes **1**, which display a much larger variation than the association rate constants: 1.2×10^7 s^{-1} (**1f**) > 1.8×10^6 s^{-1}(**1d**) > 1.0×10^6 s^{-1} (**1e**) > 4.4×10^5 s^{-1} (**1a**) > 3.7×10^5 s^{-1} (**1c**). Interestingly, this order is the reverse of that established for the hydrophobicity (cf. binding constants). This factor may be a common denominator of the dissociation rate constants.

Conclusions

Thermodynamic, kinetic, and structural aspects of complexation by cyclodextrins (CDs) play an essential role in the understanding of their functions and for the development of prospective applications. A fast kinetics, for example, is desirable for catalytic activity, and a regulated release of the guest is essential in drug delivery. On the other hand, a strong and selective binding may be of interest for analytical or environmental purposes. Finally, the solution structures are intimately related to molecular recognition, and the specific location of functional groups in the CD cavity, in particular in solution, may be the prerequisite for enzymatic specificity. A pertinent example is that of ester hydrolysis, where the secondary hydroxyl rim catalyzes the reaction at the acyl site.[74,75]

We have provided herein a comprehensive data set for substituent effects on the binding constants and association rate constants for complexation of azoalkanes **1** by β-CD and the solution structures of the resulting complexes (co-conformations). This joint study of structural, kinetic, and thermodynamic effects was made possible by the application of several independent spectroscopic techniques in aqueous solution. Azoalkanes **1** serve as molecular probes, which can be examined by UV, time-resolved and steady-state fluorescence, ICD, and NMR. We have shown that the structures of the CD complexes of azoalkanes **1**, which can be examined by ICD and NMR, are mainly governed by steric effects and hydrogen bonding. An unexpected structural variation, signaled by the inversion of the ICD sign, was observed for the hydroxyl, amino, and ammonium substituents. The complex stability appears to be dominated by an interplay between hydrophobic and specific structural effects, while the association rate constants, which can be determined by fluorescence decay, are relatively insensitive to substitution. The estimated dissociation rate constants show a larger variation and appear to be correlated with the hydrophobicity of the guest.

Acknowledgment. This work was supported by the Swiss National Science Foundation (projects 620-58000 and 4047-057552) within the Swiss National Research Program "Supramolecular Functional Materials" and MHV grant 2134-62567.00 for G.G.

JA011866N

(73) Liao, Y.; Bohne, C. *J. Phys. Chem.* **1996**, *100*, 734−743.

(74) VanEtten, R. L.; Sebastian, J. F.; Clowes, G. A.; Bender, M. L. *J. Am. Chem. Soc.* **1967**, *89*, 3242−3253.

(75) Tee, O. S.; Bozzi, M.; Hoeven, J. J.; Gadosy, T. A. *J. Am. Chem. Soc.* **1993**, *115*, 8990−8998.

(76) Rodger, A.; Nordén, B. *Circular Dichroism and Linear Dichroism*; Oxford University Press Inc.: New York, 1997.